Anisotropy of Cosmic Acceleration

Wen Zhao[1], Puxun Wu[2] and Yang Zhang[1]

[1]*Key Laboratory for Researches in Galaxies and Cosmology, Department of Astronomy,*
University of Science and Technology of China, Hefei, Anhui, 230026, China
[2]*Center for Nonlinear Science and Department of Physics,*
Ningbo University, Ningbo, Zhejiang, 315211, China
(Dated: May 17, 2013)

In this paper, we study the anisotropy of cosmic acceleration by dividing the Union2 Type Ia supernova dataset into 12 subsets according to their positions in Galactic coordinate system. In each region, we derive the deceleration parameter q_0 as the diagnostic to quantify the anisotropy level in the corresponding direction, and construct q_0 anisotropic maps by combining these q_0 values. In addition to the monopole component, we find the significant dipole effect in the q_0-maps with the amplitude $A_1 = 0.466^{+0.255}_{-0.205}$, which deviates from zero at more than 2-σ level. The direction of the best-fit dipole is ($\theta = 108.8°$, $\phi = 187.0°$) in Galactic system. Interesting enough, we find the direction of this dipole is nearly perpendicular to the CMB kinematic dipole, and the angle between them is 95.7°. The perpendicular relation is anomalous at the 1-in-10 level.

I. INTRODUCTION

Soon after the discovery of the accelerating cosmic expansion from the observations of Type Ia supernova (SNIa) [1, 2], a number of authors have investigated the anisotropies of the cosmic acceleration [3–19], which was motivated in several aspects: From the theoretical point of view, the anisotropy may arise in some cosmological models, such as the vector dark energy models [20–24], the anisotropic equation-of-state of dark energy[25], the non-trivial cosmic topology [26–28], the statistically anisotropic primordial perturbations [29, 30] or the existence of a large-scale primordial magnetic field [31–33]. And also the study can be used to check the validity of the cosmological principle [34–36], to measure expected deviations from the isotropy due to various motions of Local Group [3–6], or to search for the possible systematic errors in observations and their analysis [14].

In particular, several groups [14–17, 19] have applied the hemisphere comparison method to study the anisotropy of ΛCDM, wCDM and the dark energy model with CPL parametrization, where the supernova data and the corresponding cosmic accelerations on several pairs of opposite hemispheres have been used to search for maximally asymmetric pair, and a statistically significant preferred axis has been reported. As emphasized in [15, 16], although this method optimizes the statistics due to the large number of supernovae in each hemisphere, it has lost all information about the detailed structure of the anisotropy.

In this paper, we shall extend this issue to investigate the cosmic acceleration in different parts of the whole sky, and study the possible existence of anisotropy. To do it, we take use of the Union2 dataset [37], and divide them into 12 parts according to their positions in Galactic coordinate system. Among them, six regions are useless and masked in the investigation due to the lack of supernova data. In each unmasked region, we study the cosmic acceleration by taking the deceleration parameter q_0 as the diagnostic, and find the significant difference for different regions. We extract the lowest multipole components, i.e. monopole and dipole, in this anisotropic map, and find that the monopole amplitude is $A_0 = -0.750^{+0.122}_{-0.172}$, which is consistent with other observations, and shows the present acceleration of cosmic expansion. Meanwhile, we find the significant dipole, and the amplitude is $A_1 = 0.466^{+0.255}_{-0.205}$, which deviates from zero in more than 2-σ confident level. Interesting enough, the direction of the best-fit dipole is at ($\theta = 108.8°$, $\phi = 187.0°$) [64], which is nearly perpendicular to CMB kinematic dipole, and the angle between these two dipole directions is 95.7°. This implies that the origin of the anisotropy of cosmic acceleration may connect with the CMB kinematic dipole.

The paper is organized as follows. In the next section we give a general introduction to the analysis method, and apply to wCDM model fitted by the Union2 dataset. In this section, we focus on the monopole and dipole components, especially the direction of dipole, and compare with CMB kinematic dipole. Sec. 3 gives our conclusions.

II. ANISOTROPY OF COSMIC ACCELERATION

In this paper we take use of the Union2 dataset [37], which contains 557 type Ia SNIa data and uses SALT2 for SNIa light-curve fitting, covering the redshift range $z = [0.015, 1.4]$ and including samples from other surveys, such as CfA3 [38], SDSS-II Supernova Search [39] and high-z Hubble Space Telescope. The direction distribution of the supernovae in Galactic coordinate system
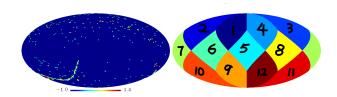
FIG. 1: Left Panel: The distribution of the SNIa in Galactic coordinate system, where the color indicates the redshift of SNIa. Right Panel: The whole sky is divided into 12 equal-area regions.

is presented in Fig. 1 (left panel) [7–9].

In order to investigate the cosmic acceleration in different directions, in principle we can divide the total supernovae into a number of groups according to their positions and redshifts. Limited by the total number of the SNIa, in this paper we shall ignore the possible redshift effect of the anisotropy. HEALPix is a genuinely curvilinear partition of the 2-dimensional sphere into exactly equal area quadrilaterals of varying shape, which is advantageous since sky signals are sampled without regional dependence [40]. The base-resolution comprises 12 pixels in three ring around the poles and equator. The resolution of the grid is expressed by the parameter Nside. In this paper, we adopt the lowest resolution with Nside=1 due to the fact that the total number of SNIa is not too large. The 12 regions are shown in Fig. 1 (right panel). We find that the distribution of SNIa in the sky is not isotropic. In Regions 5, 6, 7, 8, i.e. Galactic plane, the numbers of SNIa are very smaller (i.e. $N_{\rm sn} = 1$ in Region 5, $N_{\rm sn} = 7$ in Region 6, $N_{\rm sn} = 11$ in Region 7, $N_{\rm sn} = 4$ in Region 11). In addition, we also find that $N_{\rm sn} = 22$ in Region 1, and $N_{\rm sn} = 5$ in Region 12. So in the following discussion, we will not use these six regions, because of the small numbers of SNIa. In Table I, we list the values of $N_{\rm sn}$ in the other six regions, which will be used for the analysis.

In each region, we fit the SNIa data by minimizing the $\chi_{\rm sn}^2$ values of the distance modulus. The $\chi_{\rm sn}^2$ for SNIa is obtained by comparing theoretical distance modulus $\mu_{th}(z) = 5 \log_{10}[d_L(z)] + \mu_0$, where $\mu_0 = 42.384 - 5 \log_{10} h$ is a nuisance parameter, with observed μ_{ob} of supernovae:

$$\chi_{\rm sn}^2 = \sum_{i=1}^{N_{\rm sn}} \frac{[\mu_{th}(z_i) - \mu_{ob}(z_i)]^2}{\sigma^2(z_i)}. \quad (1)$$

The expressions of $d_L(z)$ and $H(z)$ depend on the cosmological model. In this paper we consider the flat Friedmann-Lemaitre-Robertson-Walker Universe and the wCDM model. So one has

$$d_L(z) = (1+z) \int_0^z \frac{H_0}{H(z')} dz', \quad (2)$$

and

$$H^2(z) = H_0^2[\Omega_m(1+z)^2 + (1-\Omega_m)(1+z)^{3+3w}]. \quad (3)$$

The nuisance parameter μ_0 can be eliminated in the following way. We expand $\chi_{\rm sn}^2$ with respect to μ_0 [41]:

$$\chi_{\rm sn}^2 = C_2 + 2C_1\mu_0 + C_0\mu_0^2, \quad (4)$$

where

$$C_k = \sum_i \frac{[\mu_{th}(z_i; \mu_0 = 0) - \mu_{ob}(z_i)]^k}{\sigma^2(z_i)}, \quad (k = 0, 1, 2).$$

Eq. (4) has a minimum as follows,

$$\tilde{\chi}_{\rm sn}^2 = \chi_{\rm sn,min}^2 = C_2 - C_1^2/C_0, \quad (5)$$

which is independent of μ_0. Actually, the difference between $\tilde{\chi}_{\rm sn}^2$ and the marginalized $\chi_{\rm sn}^2$ is just a constant [41]. In the following analysis, we will adopt $\tilde{\chi}_{\rm sn}^2$ as the goodness of fitting between theoretical model and SNIa data.

Similar to [17], we use the deceleration parameter q_0 as the diagnostic of the cosmic acceleration. In the wCDM model, the present value of q_0 can be expressed as

$$q_0 = \frac{1 + 3w(1 - \Omega_m)}{2}, \quad (6)$$

which is a combination of the parameters w and Ω_m. The results of the cosmological parameters Ω_m, w and the corresponding q_0 in each region are shown in Table I. Interesting, we find the significant difference for the different regions, even if the error bars are considered. For example, the absolute values of q_0 are quite small in Regions 10 and 11, but fairly large in Regions 2, 4, 9. The similar difference also exists for the parameters Ω_m and w. These are the clear indications of the anisotropy of the cosmic acceleration.

As the first step to quantify the anisotropy, we use the best-fit q_0 values as the diagnostic, which is shown in Fig. 2 (upper panel). In order to describe the 2-dimensional anisotropic map, it is convenient to expand it over the spherical harmonics as follows:

$$q_0(\theta, \phi) = \sum_{l=0}^{l_{\rm max}} \sum_{m=-l}^{l} a_{lm} Y_{lm}(\theta, \phi), \quad (7)$$

where Y_{lm} are the spherical harmonics, and a_{lm} are the corresponding multipole coefficients. In this paper, due to the low resolution of the anisotropic map, we only consider the lowest multipoles: monopole with $l = 0$ and dipole with $l = 1$.

We apply the routine provided in HEALPix package to subtract the monopole and dipole components from the partial HEALPix map [40]. The fit is obtained by solving the linear system

$$\sum_{j=0}^{3} A_{ij} f_j = b_i, \quad (8)$$

and

$$b_i = \sum_{p \in \mathcal{P}} s_i(p) m(p), \quad A_{ij} = \sum_{p \in \mathcal{P}} s_i(p) s_j(p), \quad (9)$$

TABLE I: Results for $N_{\rm sn}$, Ω_m, w and q_0 in the six unmasked regions.

	Region 2	Region 3	Region 4	Region 9	Region 10	Region 11
$N_{\rm sn}$	82	62	35	104	181	43
Ω_m	$0.330^{+0.093}_{-0.150}$	$0.000^{+0.289}$	$0.301^{+0.148}_{-0.301}$	$0.417^{+0.104}_{-0.284}$	$0.133^{+0.226}_{-0.133}$	$0.152^{+0.245}_{-0.152}$
w	$-1.270^{+0.453}_{-0.610}$	$-0.755^{+0.095}_{-0.650}$	$-1.291^{+0.653}_{-1.191}$	$-1.423^{+0.756}_{-0.949}$	$-0.742^{+0.193}_{-0.483}$	$-0.662^{+0.222}_{-0.659}$
q_0	$-0.777^{+0.278}_{-0.390}$	$-0.616^{+0.328}_{-0.302}$	$-0.853^{+0.396}_{-0.740}$	$-0.745^{+0.393}_{-0.544}$	$-0.464^{+0.140}_{-0.239}$	$-0.342^{+0.273}_{-0.390}$

where $\mathcal{P}$ is the set of valid, unmasked pixels, and $m(p)$ is the input map. $s_0(p) = 1$ and $s_1(p) = x$, $s_2(p) = y$, $s_3(p) = z$ are respectively the monopole and dipole templates. The output monopole and dipole are respectively,

$$m_{\rm monopole}(p) = f_0, \quad m_{\rm dipole}(p) = \sum_{i=1}^{3} f_i s_i(p). \quad (10)$$

Applying to the q_0-map in Fig. 2 (upper panel), we obtain the fit monopole $A_0 = -0.674$, which is equivalent to the average decelerating parameter in the whole sky. This value clearly shows that the present Universe is in an accelerating expansion stage, which is consistent with other results [42, 43].

However, if we subtract this fit monopole from the q_0-map, the residual is still significant, which has the similar amplitude with the monopole component (see the middle panel in Fig. 2). This shows that the anisotropy of q_0-map is quite important, which is also the motivation of our discussion in this paper. The lowest anisotropic component is the dipole. The dipole is described by the amplitude A_1 and the direction (θ, ϕ) in Galactic coordinate system. For the q_0-map, we get the fit dipole with the parameters $(A_1 = 0.349, \theta = 127.4°, \phi = 211.5°)$, which is plotted in left panel of Fig. 3. We find that the amplitudes of dipole and monopole are the same order. If subtracted both monopole and dipole from the q_0-map, we find the residual becomes very small, which is clearly shown in the lower panel in Fig. 2. This implies that the main anisotropic component in q_0-map is contributed by the dipole component.

Recently, a few puzzling large-scale cosmological observations have been reported to challenge the standard model, which includes the alignment of the low multipoles of CMB temperature and polarization anisotropies [44–46], the parity asymmetry of CMB power spectrum [47, 48], the large-scale velocity flows [49, 50] and the large scale alignment in the QSO optical polarization data [51, 52]. Especially, it was noticed that these anomalies are all connected with the CMB kinematic dipole in some sense [15, 16]. Even the preferred axis of cosmic acceleration detected in [14–17, 19] by using the hemisphere comparison method is also claimed to align with the CMB kinematic dipole. Here, we shall also compare the direction of the derived dipole component with that of CMB kinematic dipole, which is $(A_1 = 3.35\text{mK}, \theta = 41.74°, \phi = 263.99°)$ [53, 54] (see right panel in Fig. 3). Note that this dipole component was derived from
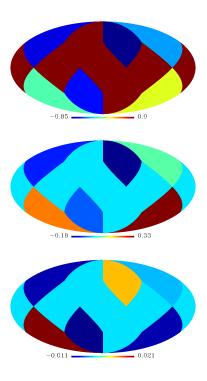

FIG. 2: Upper Panel: The best-fit q_0 values in different regions. Middle Panel: The monopole component is subtracted in upper panel. Lower Panel: Both monopole and dipole are subtracted in upper panel.

the WMAP data, and has been used by Planck mission for the calibration [55]. The angle between these two dipoles is $\alpha = 97.6°$. So we find that, instead of alignment, these two dipoles are nearly perpendicular with each other. Actually, the maximum axis reported by Antoniou and Perivolaropoulos in [15, 16] is $(\theta = 108°, \phi = 129°)$ [65]. And the angle between this direction and the CMB kinematic dipole direction is $132.7°$. The different between these two results may be caused by the different direction resolutions of the methods.

Now, let us discuss the monopole and dipole components in the general q_0-map, instead of those in the best-fit map. According to the q_0 likelihood functions in the unmasked regions, we generate $1,000,000$ random samples of $\{q_0^2, q_0^3, q_0^4, q_0^9, q_0^{10}, q_0^{11}\}$, where q_0^i stands for the q_0 in the i-th region. For each dataset, we derive the corresponding monopole and dipole, and calcu-
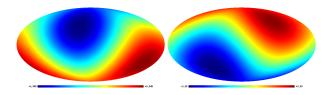
FIG. 3: Left Panel: The dipole component in the upper panel of Fig. 2. Right Panel: CMB kinematic dipole with the unit: mK.

late the 1-dimensional likelihood functions for A_0 and A_1 parameters, which are shown in Fig. 4. We find that $A_0 = -0.750^{+0.122}_{-0.172}$, which is smaller than zero in more than 5-σ confident level. So the present Universe is in an accelerating stage. Interesting enough, we also find that $A_1 = 0.466^{+0.255}_{-0.205}$, i.e. the amplitude of dipole is non-zero at more than 2-σ level. So again, we find that the dipole effect is quite significant.

In order to study the direction of the dipole component, in Fig. 5 we plot the likelihood distribution in 2-dimensional space (left panel), and the corresponding best-fit value is ($\theta = 108.8°$, $\phi = 187.0°$). It is very interesting to find that the angle between this best-fit dipole and CMB kinematic dipole is $\alpha = 95.7°$. Again, we find that these two dipoles are nearly perpendicular with each other. In the right panel, we plot 1-σ with yellow region and 2-σ with cyan region. For comparison with CMB kinematic dipole, in this figure we also plot the region with black line, which is exactly perpendicular to CMB kinematic dipole. We find this black line excellently crosses the centers of 1-σ and 2-σ regions, which is consistent with the above results. The 1-dimensional likelihood functions for θ and ϕ are also shown in Fig. 4, which correspond to the constraints of $\theta = 113.9^{+23.9}_{-17.2}$ and $\phi = 190.6^{+46.6}_{-30.3}$.

In order to quantify the perpendicular relation between these two dipole directions $\hat{n}_1$ (the best-fit dipole of cosmic acceleration) and $\hat{n}_2$ (CMB kinematic dipole), similar to [56], we can define the dot product $\hat{n}_1 \cdot \hat{n}_2$. Under the null hypothesis that these two dipoles are statistically independent, with the unit vectors $\hat{n}_1$ and $\hat{n}_2$ being independently drawn from a distribution where all directions are equally likely. This means that the dot product $|\hat{n}_1 \cdot \hat{n}_2|$ is a uniformly distributed random variable on the interval $[0, 1]$. By using the values of $\hat{n}_1$ and $\hat{n}_2$, we get $|\hat{n}_1 \cdot \hat{n}_2| = 0.10$, corresponding to a separation of 95.7°. So a perpendicular this good happens by chance only once in $1/0.10 \simeq 10$.

In the end of this section, although we will not detailedly study the physical mechanism of the perpendicular relation in this paper, we could provide some possible reasons for this coincidence problem. Similar to other puzzles in the large-scale observations [44–52] (see [57] as a review), these anomalies may be the indications of the non-trivial cosmic topology, such as the Bianchi type models [26, 27]. On the other hand, as mentioned by
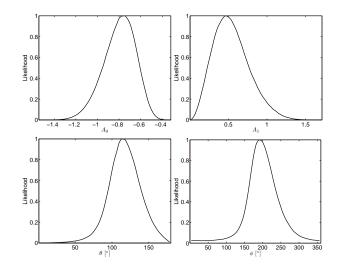

FIG. 4: The 1-dimensional likelihood functions for A_0, A_1, θ and ϕ.
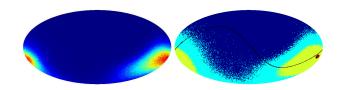

FIG. 5: Left Panel: The distribution of the dipole directions in Galactic coordinate system. Right Panel: The best-fit direction of dipole (red spot), 1-σ region (yellow), and 2-σ region (cyan). The black line shows the plane, which is perpendicular to CMB kinematic dipole.

some authors [7–9, 14], these coincidences may also hint some unsolved systematical errors in observations or data analysis.

III.   CONCLUSIONS AND DISCUSSIONS

Recently, the anisotropy of cosmic acceleration has attracted great attention, which may be caused by the non-trivial cosmic topology or some residuals of observational errors. In this paper, by using the Union2 SNIa dataset at different regions in the whole sky, we investigated the dependence of cosmic acceleration on the directions in the Galactic coordinate system, where the deceleration parameter q_0 has been used as the diagnostic to quantify the anisotropy level.

In the anisotropic q_0-maps, we find the significant dipole effect with the amplitude $A_1 = 0.466^{+0.255}_{-0.205}$, which deviates from zero at more than 2-σ level. This study also shows that the direction of the dipole trends to be perpendicular to CMB kinematic dipole. The best-fit dipole direction is ($\theta = 108.8°$, $\phi = 187.0°$), and the angle between this direction and that of CMB kinematic dipole is 95.7°. We find the perpendicular relation between these

two dipoles is anomalous at the 1-in-10 level.

It is important to mention that as more and more supernovae data will be released in the near future [58], the much more details of the anisotropy on cosmic acceleration could be revealed (including the higher multipoles with $l \geq 2$ and the dependence of redshift), which would be helpful to resolve the origin of anisotropy on cosmic acceleration, and the association with CMB kinematic dipole.

Recently, the new release of the Planck observations on the CMB temperature anisotropy confirmed the alignment of the CMB quadrupole and octupole. And this particular direction is nearly aligned with CMB kinematic dipole direction [59]. At the same time, the discontinuous distribution of power in the hemispheres on the sky was also been confirmed. All these show that we have the evidence for a break in isotropy. In order to solve these problems, a phenomenological dipole modulation may be needed [59, 60]. Since all these directional anomalies, as well as the alignment problems of the cosmic acceleration anisotropy discussed in this paper, the parity asymmetry of CMB power spectrum [47], the large-scale velocity flows [49] and the large scale alignment in the QSO optical polarization data [51] are connected with the CMB kinematic dipole and/or the ecliptic plane. We expect a single dipole modulation mechanism could solve all these puzzles.

Several works have suggested that this kind of modulation could be caused by the non-trivial topology of the Universe, such as the anisotropic global Bianchi VIIh geometry [61], the Randers-Finsler geometry [62], or the multi-stream inflation [63]. However, if they have the cosmological origin, it is very difficult to answer: Why the special direction is related to the current motion direction of the Earth, i.e. the CMB kinematic dipole. So, in our view, we would rather believe that these problems should be caused by some unsolved systematical errors in observations or data analysis. In any case, the much more detailed investigations on this kind of directional anomalies are necessary.

[1] S. Perlmutter, G. Aldering, G. Goldhaber, et al., Astrophys. J. **517**, 565 (1999).
[2] A. G. Riess, A. V. Filippenko, P. Challis, et al., Astron. J. **116**, 1009 (1998).
[3] C. Gordon, K. Land, and A. Slosar, Phys. Rev. Lett. **99**, 081301 (2007).
[4] C. Gordon, K. Land and A. Slosar, Mon. Not. Roy. Astron. Soc. **387**, 371 (2008).
[5] C. G. Tsagas, Mon. Not. Roy. Astron. Soc. **405**, 503 (2010).
[6] T. M. Davis, et al., Astrophys. J. **741**, 67 (2011).
[7] C. Bonvin, R. Durrer and M. A. Gasparini, Phys. Rev. D **73**, 023523 (2006).
[8] M. Blomqvist, J. Enander and E. Mortsell, JCAP **10**, 018 (2010).
[9] S. A. Appleby1 and E. V. Linde, arXiv:1210.8221.
[10] S. Gupta, T. D. Saini and T. Laskar, Mon. Not. Roy. Astron. Soc. **388**, 242 (2008).
[11] S. Gupta and T. D. Saini, Mon. Not. Roy. Astron. Soc. **407**, 651 (2010).
[12] L. Campanelli, P. Cea, G. L. Fogli and A. Marrone, Phys. Rev. D **83**, 103503 (2011).
[13] J. Colin, R. Mohayaee, S. Sarkar and A. Shafieloo, Mon. Not. Roy. Astron. Soc. **414**, 264 (2011).
[14] D. J. Schwarz and B. Weinhorst, Astron. Astrophys. **474**, 717 (2007).
[15] I. Antoniou and L. Perivolaropoulos, JCAP **1012**, 012 (2010);
[16] A. Mariano and L. Perivolaropoulos, arXiv:1206.4055.
[17] R. G. Cai and Z. L. Tuo, JCAP **1202**, 004 (2012).
[18] B. Kalus, D. J. Schwarz, M. Seikel and A. Wiegand, Astron. Astrophys. 553, A56 (2013).
[19] R. G. Cai, Y. Z. Ma, B. Tang and Z. L. Tuo, arXiv:1303.0961.
[20] C. Armendariz-Picon, JCAP **0407**, 007 (2004).
[21] W. Zhao and Y. Zhang, Class. Quant. Grav. **23**, 3405 (2006).
[22] W. Zhao and Y. Zhang, Phys. Lett. B **640**, 69 (2006).
[23] Y. Zhang, T. Y. Xia, W. Zhao, Class. Quant. Grav. **24**, 3309 (2007).
[24] T. S. Koivisto and D. F. Mota, JCAP **0808**, 021 (2008).
[25] T. Koivisto and D. F. Mota, Astrophys. J.**679**, 1 (2008).
[26] T. R. Jaffe, S. Hervik, A. J. Banday and K. M. Gorski, Astrophys. J. **644**, 701 (2006).
[27] A. Pontzen and A. Challinor, Mon. Not. Roy. Astron. Soc. **380**, 1387 (2007).
[28] P. Bielewicz and A. Riazuelo, Mon. Not. Roy. Astron. Soc. **396**, 609 (2009).
[29] C. Armendariz-Picon, JCAP **0709**, 014 (2007).
[30] A. R. Pullen and M. Kamionkowski, Phys. Rev. D **76**, 103529 (2007).
[31] M. Giovannini and M. Shaposhnikov, Phys. Rev. D **62**, 103512 (2000).
[32] T. Kahniashvili, G. Lavrelashvili and B. Ratra, Phys. Rev. D **78**, 063012 (2008).
[33] J. Kim and P. Naselsky, JCAP **0907**, 041 (2009).
[34] T. S. Kolatt and O. Lahav, Mon. Not. Roy. Astron. Soc. **323**, 859 (2001).

[35] T. Clifton, P. G. Ferreira and K. Land, Phys. Rev. Lett. **101**, 131302 (2008).

[36] T. J. Zhang, H. Wang and C. Ma, arXiv:1210.1775.

[37] R. Amanullah, et al., Astrophys. J. **716**, 712 (2010).

[38] M. Hicken, et al., Astrophys. J. **700**, 1097 (2009).

[39] J. A. Holtzman, et al., Astron. J. **136**, 2306 (2008).

[40] K. M. Gorski, E. Hivon, A. J. Banday, B. D. Wandelt, F. K. Hansen, M. Reinecke and M. Bartelman, Astrophys. J. **622**, 759 (2005).

[41] S. Nesseris and L. Perivolaropoulos, Phys. Rev. D **72**, 123519 (2005).

[42] Y. Gong and A. Wang, Phys. Rev. D **75**, 043520 (2007).

[43] P. Wu and H. Yu, JCAP **0802**, 019 (2008).

[44] K. Land and J. Magueijo, Phys. Rev. Lett. **95**, 071301 (2005).

[45] M. Frommert and T. A. Ensslin, Mon. Not. Roy. Astron. Soc. **403**, 1739 (2010).

[46] C. L. Bennett, et al., Astrophys. J. Suppl. Ser. **192**, 17 (2011).

[47] J. Kim and P. Naselsky, Astrophys. J. Lett. **714**, L265 (2010)

[48] P. Naselsky, W. Zhao, J. Kim and S. Chen, Astrophys. J. **749**, 31 (2012).

[49] R. Watkins, H. A. Feldman and M. J. Hudson, Mon. Not. Roy. Astron. Soc. **392**, 743 (2009).

[50] H. A. Feldman, R. Watkins and M. J. Hudson, Mon. Not. Roy. Astron. Soc. **407**, 2328 (2010).

[51] D. Hutsemekers, R. Cabanac, H. Lamy and D. Sluse, Astron. Astrophys. **441**, 915 (2005);

[52] D. Hutsemekers, A. Payez, R. Cabanac, H. Lamy, D. Sluse, B. Borguet and J. R. Cudell, arXiv:0809.3088.

[53] N. Jarosik, et al., Astrophys. J. Suppl. Ser. **192**, 14 (2011).

[54] G. Hinshaw, et al., Astrophys. J. Suppl. Ser. 180, 225 (2009).

[55] Planck Collaboration, arXiv:1303.5069.

[56] A. de Oliveira-Costa, M. Tegmark, M. Zaldarriaga and A. Hamilton, Phys. Rev. D **69**, 063516 (2004).

[57] L. Perivolaropoulos, arXiv:1104.0539.

[58] A. Albrecht, et al., arXiv:astro-ph/0609591.

[59] Planck Collaboration, arXiv:1303.5083.

[60] C. Gordon, W. Hu, D. Huterer and T. Crawford, Phys. Rev. D**72**, 103002 (2005).

[61] Planck Collaboration, arXiv:1303.5086.

[62] Z. Chang and S. Wang, arXiv:1303.6058.

[63] Y. Wang, arXiv:1304.0599.

[64] Throughout this paper, we use the polar coordinate (θ,ϕ) in the Galactic system, which relates to the Galactic coordinate (l, b) by $l = 90° - \theta$ and $b = \phi$.

[65] Note that, the analysis does not distinguish this direction and the opposite direction at $(\theta = 72°, \phi = 309°)$.